Challenges in Panchromatic Modelling with Next Generation Facilities
Proceedings IAU Symposium No. 341, 2018
M. Boquien, E. Lusso, C. Gruppioni & P. Tissera, eds.

doi:10.1017/S1743921319002886

The onset of star formation 250 million years after the Big Bang

Takuya Hashimoto[1,2]

[1]Department of Environmental Science and Technology, Faculty of Design Technology, Osaka Sangyo University, 3-1-1, Nagaito, Daito, Osaka 574-8530, Japan

[2]National Astronomical Observatory of Japan, 2-21-1 Osawa, Mitaka, Tokyo 181-8588, Japan
email: thashimoto@est.osaka-sandai.ac.jp

Abstract. In this IAU symposium, we present results of our recent paper, Hashimoto *et al.* (2018a) focusing on its spectral energy distribution modeling. We present spectroscopic observations of MACS1149-JD1, a gravitationally lensed galaxy originally discovered by Zheng *et al.* (2012) via the dropout technique. Using the Atacama Large Millimeter/submillimeter Array (ALMA), we detect an emission line of doubly ionized oxygen, [OIII] 88 μm, at a redshift of 9.1096±0.0006. This precisely determined redshift indicates that the red rest-frame optical colour observed with the Spitzer Space Telescope arises from a dominant stellar component that formed about 250 million years after the Big Bang, corresponding to a redshift of about 15. MACS1149-JD1 clearly demonstrates the importance and power of spectral energy distribution modeling to understand the earliest star formation history of the Universe.

Keywords. galaxies: evolution, galaxies: formation, galaxies: high-redshift, galaxies: individual (MACS1149-JD1)

1. Introduction

With the advent of the Atacama Large Millimeter/Submillimeter Array (ALMA) telescope, recent studies demonstrate how the far-infrared (FIR) fine structure line of doubly ionized oxygen ([OIII] 88 μm) is powerful to identify galaxies in the reionization epoch, redshift (z) beyond 6. In two years after the first detection of [OIII] in the reionization epoch by Inoue *et al.* (2016) at $z = 7.21$, twelve [OIII] detections at $z > 6$ are reported in the literature (Inoue *et al.* 2016; Carniani *et al.* 2017; Laporte *et al.* 2017; Marrone *et al.* 2018; Hashimoto *et al.* 2018a,b,c; Tamura *et al.* 2018; Walter *et al.* 2018). Among these, Laporte *et al.* (2017) and Tamura *et al.* (2018) have detected [OIII] in A2744_YD4 at $z = 8.38$ and MACS0416_Y1 at $z = 8.31$, respectively. Interestingly, these two $z \approx 8$ galaxies also show dust continuum detections, indicating fast growth of dust grains in the early Universe. Remarkably, Hashimoto *et al.* (2018a) have detected [OIII] at the significance level of 7.4σ in a gravitationally-lensed galaxy, MACS1149-JD1 (Zheng *et al.* 2012), at $z = 9.1096 \pm 0.0006$ using ALMA. The dust continuum emission is undetected in MACS1149-JD1. Based on VLT/X-Shooter observations, Lyα is also detected at 4.0σ. MACS1149-JD1 is the most distant object whose emission lines have been identified.

2. Spectral Energy Distribution Analyses

MACS1149-JD1 is currently the only one galaxy which has a rich data set from rest-frame UV, optical, to far-infrared at $z > 9$. A striking feature of the target is its red

Spitzer/IRAC colour. Previous to Hashimoto *et al.* (2018a), the origin of the colour was not uniquely determined: Without its precise spectroscopic redshift, the colour can be reproduced by both (1) contamination from strong nebular emission lines by young metal-poor stellar populations and (2) contamination from the Balmer break indicative of old stellar populations (Hoag et al. 2018). Understanding the IRAC colour is a key to unveil properties of MACS1149-JD1.

To build the SED of our target, we use data from the three deep *HST* images (Zheng *et al.* 2017), the deep K_s image obtained with VLT/HAWK-I (Hoag et al. 2018) as well as the deep *Spitzer*/IRAC 3.6 and 4.5 μm data (Zheng *et al.* 2017). In addition to these, we use our deep upper limit on dust continuum emission as well as our measurement of the [OIII] flux (see Table 1 of Hashimoto *et al.* 2018a). We use our own SED fitting code named PANHIT (Mawatari *et al.* 2016, Mawatari *et al.* in preparation), which is also adopted in Hashimoto *et al.* (2018b) and Tamura *et al.* (2018). For the details, we refer the readers to the website, http://www.icrr.u-tokyo.ac.jp/ mawatari/PANHIT/PANHIT.html.

We first adopted single stellar population models. We find that, with an exponentially declining star formation history (SFH), the [OIII] line flux cannot be reproduced while the HST and IRAC data points are relatively well reproduced: Under the assumption of the declining SFH, the star formation rate (SFR) at $z = 9.11$ becomes too small for the observed [OIII] flux. In the case of the constant SFR, we obtain a very large reduced χ^2 (χ^2_ν) value of $\simeq 11.4$, implying that the models are inappropriate. What is worse, we obtain the stellar age of $\simeq 500$ Myr, similar to the age of the Universe at this redshift, which we consider physically unacceptable. In the constant SFR case, one might think that the IRAC colour could be reproduced by young metal-poor models with strong nebular emission lines. Indeed, the Hβ plus [OIII] 4959 Å lines can contaminate the IRAC channel 2 at $z = 9.11$. Our nebular emission line model of Inoue (2011) accounts for extremely strong emission line cases with rest-frame equivalent widths up to EW(Hβ+[OIII] 4959 Å) ~ 1550 Å for young metal-poor stellar populations (see Figures 9 and 10 of Inoue 2011). Based on our detailed analyses, we find that the IRAC channel 2 is indeed boosted due to strong Hβ plus [OIII] 4959 Å lines in young metal-poor cases. However, the IRAC channel 1 is also boosted by nebular continuum and [OII] 3727 Å line, counterbalancing the IRAC colour. To summarize, single stellar population models cannot reproduce the observed SED.

We next considered a two stellar component SED comprising a young starburst and an old population. In order to reproduce the observed SED with as small a number of parameters as possible, we assumed constant SFRs for both components. Such assumptions are also adopted in Hashimoto *et al.* (2018b). We adopted several star formation durations for the old component, namely $\tau = 10$, 100, 200, 300, and 400 Myr. In these two component models, we can reproduce the observations with $\chi^2_\nu \sim 2.8 - 3.0$. Models with $\tau = 300$ and 400 Myr lead to a stellar age > 400 Myr at $z = 9.1$, similar to the age of the Universe at this redshift, which we consider physically unacceptable. The other three models give a similar quality fit and ages for the old stellar population ranging from 230 to 320 Myr. Due to the similarity of the physical and statistical results produced by the three remaining models, we cannot easily discriminate one over the other. For this reason, we select the $\tau = 100$ Myr model as our fiducial case but include uncertainties which reflect the standard deviation caused by the choice of a $\tau = 10$ or 200 Myr model.

Figure 1 shows our fiducial SED models, showing that all the data are well reproduced. The top, middle, and bottom panel of Figure 2 shows the SFH, mass assembly history, and the Balmer break growth, respectively, for the models with $\tau = 10$, 100, and 200

https://doi.org/10.1017/S1743921319002886 Published online by Cambridge University Press

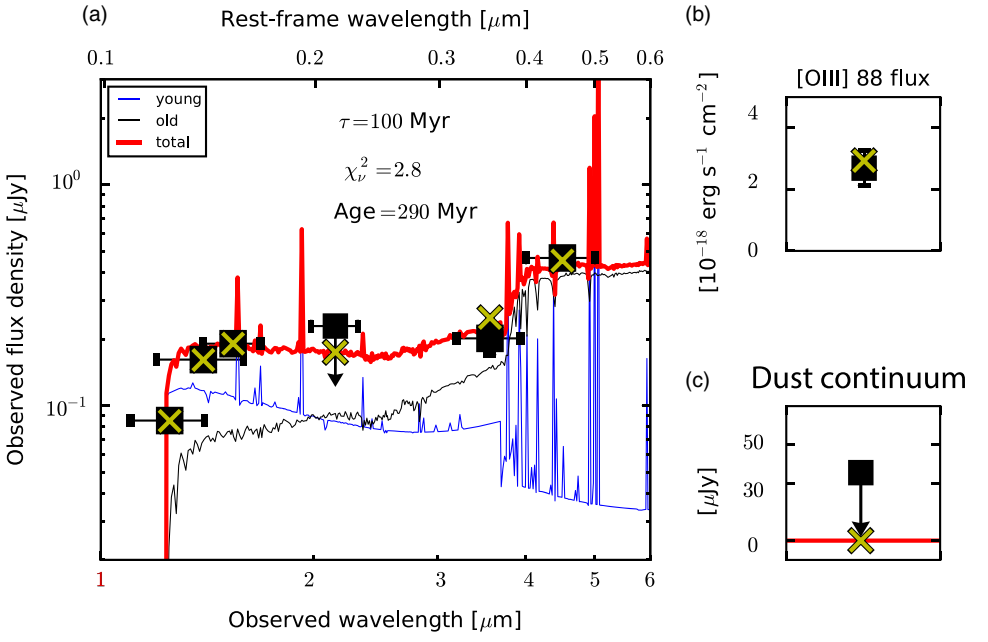

Figure 1. The SED of MACS1149-JD1 in the case of our fiducial model with $\tau = 100$ Myr (see the text for the details). In panel (a), black squares show the observations: F125W, F140W, and F160W data from *HST*, a 2σ upper limit for the K_s-band from VLT/HAWK-I, and 3.6μm and 4.5μm fluxes from *Spitzer*/IRAC. Horizontal and vertical error bars show the wavelength range of the filters and 1σ measurement uncertainties, respectively. The red solid line indicates the SED model and the corresponding magnitudes are shown via yellow crosses. Blue and black lines represent the contributions from the young and old component, respectively. In panel (b), the black square is the observed [OIII] emission line flux and its 1σ uncertainty, while the yellow cross indicates the model prediction. In panel (c), the black square shows the 2σ upper limit for the dust continuum flux density, and the yellow cross the model prediction.

Myr, demonstrating that MACS1149-JD1 has already started its first star formation as early as 250 million yeas after the Big Bang ($z \approx 15$).

3. Discussion and Summary

Our results clearly highlight the importance and power of multi-wavelength SED fitting to trace the earliest star formation history of the Universe. Very recently, Rocca-Volmerange *et al.* (2018) have analyzed the SED of three spectroscopically identified galaxies at $z \approx 8$ with Pegase.3. The authors have shown that the IRAC excess in these three galaxies are also due to the Balmer breaks. Is it possible that current bright $z \approx 8-9$ galaxies are biased against rare matured objects? Obviously, we need to increase the sample of spectroscopically identified galaxies at this epoch. *JWST* will help to investigate detailed properties of fainter galaxies at $z \approx 8-9$. It would be also interesting to examine how such Balmer breaks are common in the early Universe in simulations.

https://doi.org/10.1017/S1743921319002886 Published online by Cambridge University Press

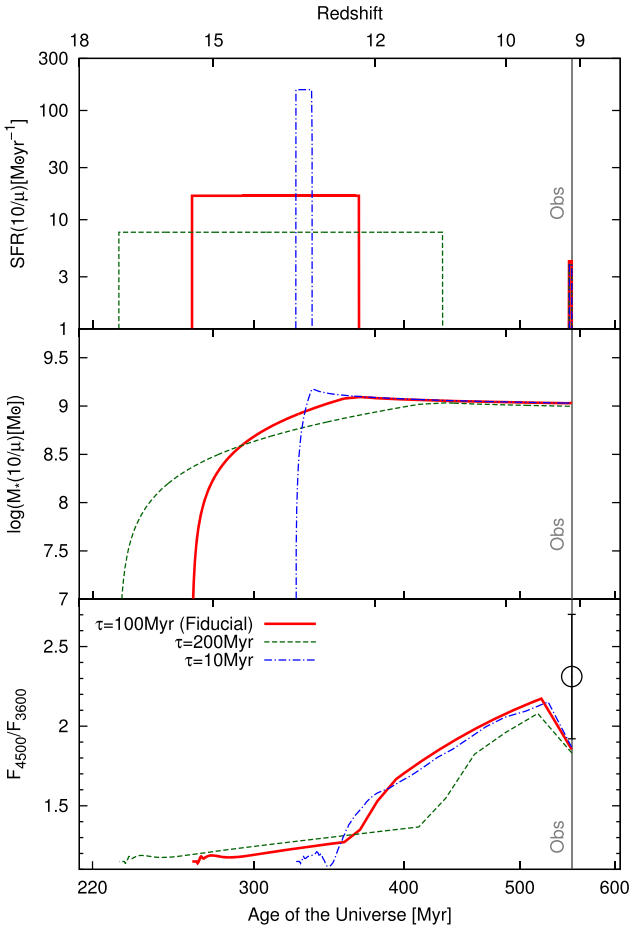

Figure 2. The star formation rate (a), stellar mass assembly (b) and Balmer break (c) as a function of redshift for three possible models. In each panel, the blue dot-dashed, green dashed, and red solid lines correspond to the models with star formation bursts of duration 10, 100, and 200 Myr, respectively. Each is capable of reproducing the Balmer break observed at $z = 9.1$ (shown by the black data point). The full SED fits shown in Figure 1 corresponds to our fiducial model corresponding to a burst of duration 100 Myr. The bulk of the stellar mass in MACS1149-JD1 observed at $z = 9.1$ was produced within a short period corresponding to the redshift interval $12 < z < 16$.

References

Hashimoto, T., Laporte, N., Mawatari, K., Ellis, R. S., Inoue, A. K., Zackrisson, E., Roberts-Borsani, G., Zheng, W., *et al.* 2018a, *Nature*, 557, 392

Zheng, W., Postman, M., Zitrin, A., Moustakas, J., Shu, X., Jouvel, S., Host, O., Molino, A., *et al.* 2012, *Nature*, 489, 406

Inoue, A. K., Tamura,Y., Matsuo, H., Mawatari, K., Shimizu, I., Shibuya, T., Ota, K., Yoshida, N., *et al.* 2016, *Science*, 352, 1559

Carniani, S., Maiolino, R., Pallottini, A., Vallini, L., Pentericci, L., Ferrara, A., Castellano, M., Vanzella, E., *et al.* 2017, *A&A*, 605, A42

Laporte, N., Ellis, R. S., Boone, F., Bauer, F., Quénard, D., Roberts-Borsani, G., Pelló, R., Pérez-Fournon, I., *et al.* 2017, *ApJL*, 837, L21

Marrone, D. P., Spilker, J. S., Hayward, C. C., Vieira, J. D., Aravena, M., Ashby, M. L. N., Bayliss, M. B., Béthermin, M., *et al.* 2018, *Nature*, 553, 51

https://doi.org/10.1017/S1743921319002886 Published online by Cambridge University Press

Hashimoto, T., Inoue, A. K., Mawatari, K., Tamura, Y., Matsuo, H., Furusawa, H., Harikane, Y., Shibuya, T., *et al.* 2018b, submitted to *PASJ*, arXiv:1806.00486
Hashimoto, T., Inoue, A, K., Tamura, Y., Matsuo, H., Mawatari, K., & Yamaguchi Y. 2018c, submitted to *PASJ*, arXiv:1811.00030
Tamura, Y., Mawatari, K., Hashimoto, T., Inoue, A. K., Zackrisson, E., Christensen, L., Binggeli, C., Matsuda, Y., *et al.* 2018, submitted to *ApJ*, arXiv:1806.04132
Walter, F., Riechers, D., Novak, M., Decarli, R., Ferkinhoff, C., Venemans, B., Bañados, E., Bertoldi, F., *et al.* 2018, *ApJ*, 869L, 22
Hoag, A., Bradač, M., Brammer, G., Huang, K.-H., Treu, T., Mason, C. A., Castellano, M., Di Criscienzo, M., *et al.* 2018, *ApJ*, 854, 39
Zheng, W., Zitrin, A., Infante, L., Laporte, N., Huang, X., Moustakas, J., Ford, H. C., Shu, X., *et al.* 2017, *ApJ*, 836, 210
Mawatari, K., Yamada, T., Fazio, G. G., Huang, J.-S., & Ashby, M. L. N. 2016, *PASJ*, 68, 46
Inoue, A. K. 2011, *MNRAS*, 415, 2920
Rocca-Volmerange, B., Hilberer, A., & Fioc, M., 2018, submitted to *A&A* arXiv:1812.04283

4. Q&A

Speaker name: Takuya Hashimoto

Questioner: Kentaro Motohara

Question: What about the exponentially declining star formation histories to reproduce the observed spectral energy distribution?

Answer: We have also performed spectral energy distribution fitting with the exponentially declining star formation histories. While the Balmer break can be reproduced, [OIII] cannot be reproduced.

https://doi.org/10.1017/S1743921319002886 Published online by Cambridge University Press